Thermotropic Polypeptides. 2. Molecular Packing and Thermotropic Behavior of Poly(L-glutamates) with Long *n*-Alkyl Side Chains

Junji Watanabe,* Hirofumi Ono, Ichitaro Uematsu, and Akihiro Abe

Department of Polymer Chemistry, Tokyo Institute of Technology, Ookayama, Meguro-ku, Tokyo, 152 Japan. *Received February 1, 1985*

ABSTRACT: A series of α-helical poly(L-glutamates), with *n*-alkyl side chains of various lengths (*n* (number of carbons in the alkyl group) = 5, 6, 8, 10, 12, 14, 16, and 18), was examined by viscoelastic, X-ray, DSC, and ORD methods. In polymers of *n* = 5, 6, and 8, the packing structures and properties were homologous with those of the familiar poly(γ-methyl L-glutamate) (*n* = 1) and varied as a simple function of side-chain length. On the other hand, they were found to be markedly altered in polymers with longer side chains (*n* ≥ 10). In these polymers, the side chains were long enough to form a crystalline phase composed of paraffin-like crystallites. The crystallization forced the α-helices to pack into the characteristic layer structure, and the crystallites were located between layers. The melting temperature, T_1, of the side-chain crystallites increased from −24 to +62 °C with increasing length of side chain from *n* = 10 to *n* = 18. Another predominant property newly induced in these polymers is the formation of thermotropic cholesteric liquid crystals. The transformation to the liquid crystalline phase took place as a first-order transition at temperature T_2, which is a little higher than T_1. The cholesteric pitches were elucidated to be a few microns at around 100 °C for poly(γ-dodecyl L-glutamate) (*n* = 12). In the intermediate temperature region between T_1 and T_2, α-helices were packed into a two-chain hexagonal lattice, which also essentially differs from a one-chain hexagonal lattice of the shorter side-chain polymers. This large lattice suggested that there may be formed a two-strand coiled-coil conformation.

Introduction

For synthetic homopolypeptides such as poly(L-glutamates), attention was initially directed to the study of the conformatioin adopted by the main chain. The conformation has appeared in various forms depending on the kind of amino acid unit and, sometimes, on their substituted side chains.[1,2] It is well-known that poly(L-glutamates) form a stable α-helical conformation even if the substituted side chains are altered. This fact makes it easy to examine the influence of side chains on the packing structure of α-helices and related properties. For this reason, intensive studies have been so far performed for a family of poly(L-glutamates).[3-13]

In such a poly(L-glutamate), a simple question arises as to what kind of properties are newly induced if long alkyl groups are attached to the side chain. As one of the new properties, paraffinic side chains may allow the polymer to be dissolved in hydrocarbons such as hexane and cyclohexane, since there is sound evidence that the solubility of α-helices in a variety of solvents is conditioned by the nature of the side chains. In practice, Smith et al.[14] have reported the solubility of poly(γ-dodecyl L-glutamate) in hydrocarbons. The use of such nonpolar solvents will provide a more tractable system for the study of the solution properties of α-helical polypeptides.

We also have some interest in new properties that are to be expected in solid-state films. The first interest concerns whether the long paraffinic side chains, in this particular case sticking out of a rigid α-helical main chain, can crystallize or not. In connection with this aspect of side-chain crystallization, Kaufman et al.[15] initially showed that long *n*-alkyl side chains of polymers based on acrylic and methacrylic acids can pack into paraffin-like crystallites. Since this study, many reseachers have been engaged in this problem and have reached the conclusion that the part of the side chain extending beyond eight or nine methylene groups participates in crystallization and that crystallites are well formed irrespective of the main-chain conformation.[16-20] In α-helical poly(L-glutamates), it is far from obvious how the side chains attached to a rigid α-helical backbone can pack so as to form crystallites of substantial size.

Another interesting point arises concerning the properties of films when the side chains are melted or amorphous. For long side chains in the amorphous state, one can envisage that the outer part of the side chain may attain the fast motion as a liquid paraffin in contrast with the limited motion of the inner part of the side chain in the vicinity of the main-chain helix. Such a liquid-like motion of side chains would reduce the interaction between neighboring molecules, and so the motion of each α-helix would be decoupled from those of surrounding α-helices. Thus, it is plausible that the long-side-chain polymers will exhibit different thermal behavior from that of the shorter side-chain polymers. More recently, Watanabe et al.[21] found that poly(γ-methyl D-glutamat-*co*-γ-hexyl D-glutamates) with the intermediate hexyl contents exhibit thermotropic cholesteric liquid crystal behavior. The nature of this novel liquid crystal has been explained in the same manner as for their lyotropic liquid crystals,[22,23] on the assumption that the terminal parts of the side chains in hexyl residues act like solvents. This study leads to the suggestion that thermotropic liquid crystals, as one of the new properties, may be achieved in long-side-chain polymers.

In this paper, we prepared homologous poly(L-glutamates) with *n*-alkyl side chains of various lengths. These polymers are shown by the following general structure:

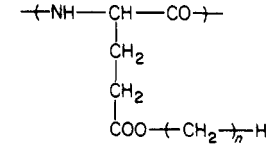

n = 5, 6, 8, 10, 12, 14, 16, 18

where *n* is defined here as the number of methylene units of the alkyl group. With the objective of seeking the new properties speculated above, we performed a study of structure and properties exhibited by the films of these polymers.

Experimental Section

Materials. A series of poly(γ-*n*-alkyl L-glutamates) was syn-

0024-9297/85/2218-2141$01.50/0

Table I
Characteristics of Poly(γ-*n*-alkyl L-glutamates)

polymer	η_{inh}, dL/g	transition temp, °C: viscoelastic method T_γ	T_β	T_α	T_1	T_2	DSC method T_1	T_2
PG-5-E	0.98	−162	−21	130				
PG-6-E	0.96	−157	−35	110				
PG-8-E	0.94	−151	−36	45				
PG-8-N	0.35	−151	−37	42				
PG-10-E	0.78	−147				35	−24	30
PG-10-N	0.46						−26	30
PG-12-E	0.62	−142			22	50	16	51
PG-12-N	0.34						15	50
PG-14-E	0.35	−132			40	60	41	61
PG-16-E	0.20	−128			55	65	54	64
PG-18-E	0.06	−122			60		62	

thesized by ester-exchange reactions between poly(γ-methyl L-glutamate) (M_v = 100 000) and the corresponding *n*-alkyl alcohols. Each reaction was carried out in 1,2-dichloroethane with *p*-toluenesulfonic acid as a catalyst at 60 °C.[24] The complete replacement of methyl groups by *n*-alkyl groups was confirmed by the NMR spectra. Poly(γ-*n*-octyl L-glutamate), poly(γ-*n*-decyl L-glutamate), and poly(γ-*n*-dodecyl L-glutamate) were also synthesized by the conventional NCA method.[14,25] The polymerization of NCA was carried out in dichloromethane with triethylamine as an initiator.

Table I lists the polymers synthesized and their intrinsic viscosities, which were determined in dichloroacetic acid solutions by using an Ubbelohde viscometer. All of the polymers are designated by the letter PG followed by the number of carbons in the side-chain alkyl group, *n*. The preparation methods are distinguished by the additional letters E and N for ester exchange and NCA, respectively. With respect to the degree of polymerization, one can suppose that the polymers prepared by the ester-exchange method have a similar degree of polymerization to that of the original poly(γ-methyl L-glutamate), which is around 700. Nevertheless, there is a great reduction of intrinsic viscosity with increase of *n*. This signifies that the common equation representing the relationship between viscosity and molecular weight cannot be applied for all polymers. The intrinsic viscosities thus allow only a relative comparison of molecular weight in the same kind of polymer. In this comparison, we notice that the molecular weight of the NCA polymer is lower than that of the ester-exchange polymer in PG-8, PG-10, or PG-12. The packing structure and properties were not essentially altered between polymers prepared by each method, so we refer below to the data of a series of polymers prepared by the ester-exchange method unless additional comments are noted.

All of the films examined here were prepared by casting the solutions in chloroform at room temperature. The IR spectra of solid films indicated that all polymers assume a right-handed α-helical conformation in this experimental temperature range.

Measurements. Dynamic mechanical measurements in the temperature range from −170 to +200 °C were made at frequencies of 110, 35, 11, and 3.5 Hz with a Rheovibron viscoelastometer Model DDV-II (Toyo Baldwin Co., Ltd.). DSC measurements were performed with a Perkin-Elmer DSC-II calorimeter. The samples were examined at a scanning rate of 10 °C/min. Wide-angle X-ray patterns were recorded with a flat-plate camera using a Rigaku-Denki X-ray generator with Ni-filtered Cu Kα radiation. The samples for this experiment were sealed in a glass capillary tube and heated at the desired temperature by a heater that could be maintained to within 1 °C. ORD curves were obtained by using a Jasco automatic recording spectrometer Model J-20 in the wavelength range from 300 to 700 nm. Densities of films were determined by flotation in aqueous KBr solutions.

Results and Discussion

A. Transition Temperatures of Polymers. We first consider the transition temperatures, which were determined by viscoelastic and DSC measurements. In Figure 1a are shown the dynamic mechanical tan δ and *E'* data measured for the first series of polymers with the shorter side chains of $n \leq 8$. This figure shows that the polymers

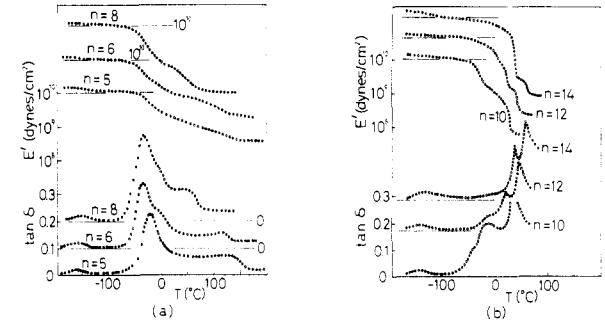

Figure 1. Temperature dependence of tan δ and *E'* measured at 110 Hz: (a) first species of polymers with $n \leq 8$; (b) second series of polymers with $n \geq 10$. The curves, with the exception of the polymer at the bottom, have been displaced upward on the ordinate axis.

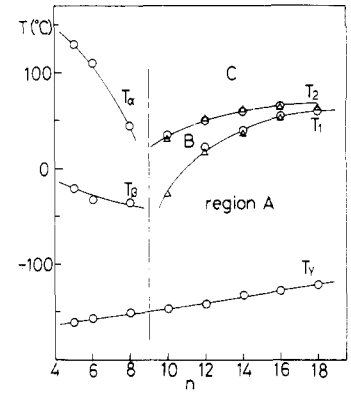

Figure 2. Dependence of transition temperatures upon the number of carbons in the side-chain alkyl group (*n*). Circles and triangles are based on dynamic mechanical and DSC data, respectively.

in this series exhibit similar dynamic mechanical properties, which are characterized by three relaxations called here γ-, β-, and α-relaxations in order of increasing temperature. In showing β- and α-relaxations these polymers are analogous to the familiar poly(γ-methyl L-glutamate) (PG-1) although the γ-relaxation is absent in the latter. The transition temperatures indicating the tan δ peak maxima, T_γ, T_β, and T_α, are listed in Table I and plotted against *n* in Figure 2.

For the lowest γ-relaxation located around −150 °C, the transition temperature increases gradually with the side-chain length. The apparent activation energies are around 10 kcal/mol of residue. These characteristics are quite similar to those of the γ-relaxation observed in a series of methacrylate polymers with corresponding *n*-alkyl side chains.[26] The γ-relaxation has been attributed to the local twisting motions of the terminal alkyl groups of the side

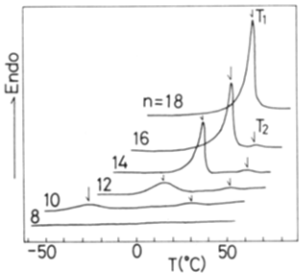

Figure 3. DSC thermograms of polymers on heating.

chains.[26,27] The β-relaxation is well-known to be due to the motion of the entire side chain. The transition temperature, T_β, decreases from 0 °C for PG-1[3] to −36 °C for PG-8, and the magnitude of the relaxation strength increases with increasing n, signifying the direct effect of the side-chain length. The highest α-relaxation is caused by the rotational and translational motions of main-chain helices with respect to their long axes, which have been predicted by an X-ray diffraction study of PG-1.[28,29] This transition is also sensitive to the side-chain length so that T_α decreases drastically from 185 °C for PG-1[3] to 45 °C for PG-8 with increasing side-chain length.

Figure 1b shows the dynamic mechanical data for another series of polymers with longer side chains than n = 10. As is typically observed for PG-14, the dynamic mechanical properties of this series of polymers are altered in some respects from those of the polymers in the first series. The appearance of the lowest γ-relaxation is consistent, but tan δ peaks due to β- and α-relaxations disappear, being replaced by two other kinds of sharp peaks, which are located in a different temperature range. The temperatures of these peaks, assigned here as T_1 and T_2, are also plotted against the carbon number in Figure 2. As can be seen in this figure, T_1 and T_2 fall on a set of curves different from the curves of T_β and T_α and increasing with side-chain length. From further inspection of dynamic mechanical data of Figure 1, one notices that the tan δ peaks at T_1 and T_2 are accompanied by an abrupt drop of the storage modulus E' while the β- and α-relaxations exhibit a moderate decrease of E'. Our experience suggests that such an abrupt drop of E' may be associated with a first-order transition.[13,30] In fact, DSC measurements have offered two kinds of first-order transitions for this class of polymers. The DSC data are shown in Figure 3, where DSC thermograms on heating are presented for polymers PG-8 to PG-18. The first-order transitions are reproducible on heating and cooling, and their peak temperatures on heating correspond well to T_1 and T_2 detected by dynamic mechanical methods, as found in Table I or in Figure 2.

In summary, there is a critical length of side chain between n = 8 and 10 in which the thermal properties of polymers are markedly altered. In the following sections, we will show the packing structure of α-helices and the related properties in each series of polymers.

B. Structure and Properties of PG-*n* for $n \leq 8$. A representative X-ray photograph of this class of polymers is shown for PG-8 in Figure 4a. As listed in Table II, the observed reflections are assigned to the hexagonal lattice with $a = b = 17.1$ Å, $c = 27$ Å, and $\gamma = 120°$. Similar hexagonal lattices are observed for PG-1,[3] PG-5, and PG-6, which have dimensions of $a = b = 12.0$, 15, and 15.5 Å, respectively. Sasaki et al.[9,10] have reported that the intermediate polymers, PG-2, PG-3, and PG-4, indicate somewhat different patterns. In this limited discussion, however, the difference does not seem to be essential, since the patterns are assigned to the monoclinic lattices slightly distorted from the hexagonal one. The spacings of the 100 reflections in the hexagonal lattices are plotted as a function of n in Figure 5. They increase along a smooth curve with side-chain length. The calculated densities based on X-ray data correspond well to the observed densities, which decrease with the side-chain length, as shown in Figure 6. The decrease in density reflects the

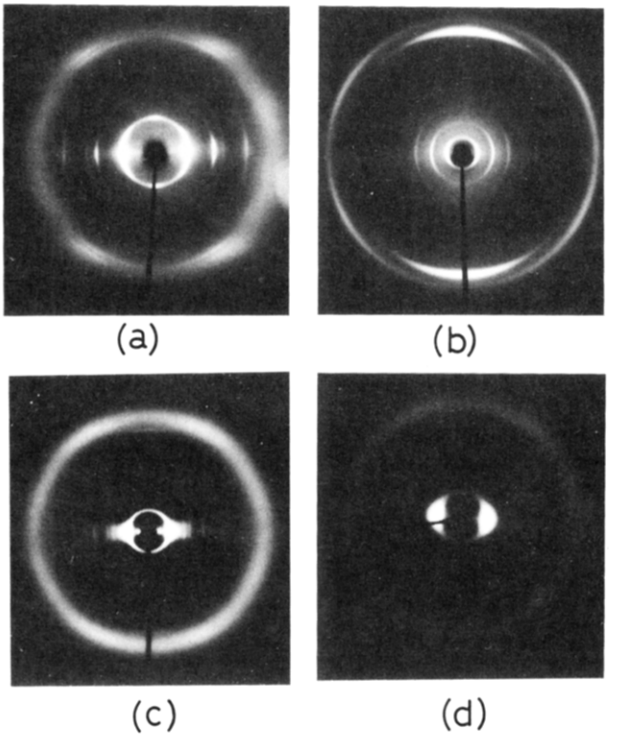

Figure 4. X-ray patterns: (a) PG-8-N at room temperature; (b) PG-18-E at room temperature (in region A); (c) PG-12-N at room temperature (in region B); (d) PG-12-N at 75 °C (in region C).

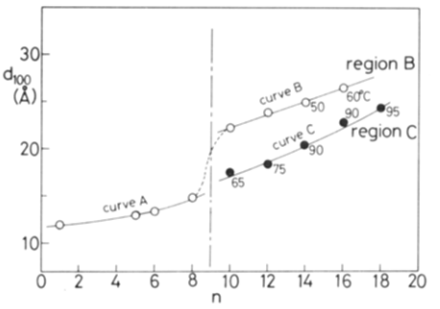

Figure 5. Variation of spacing of the first equatorial reflection (d_{100}) as a function of n. For polymers of $n \geq 10$, the open and filled circles show the data in regions B and C, respectively. The measured temperatures are noted close to the circles; no notation means room temperature.

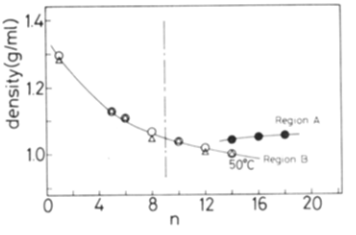

Figure 6. Variation of the observed densities as a function of n. For polymers of $n \geq 10$, the filled and open circles show the data in regions A and B respectively. Triangles indicate the calculated densities based on X-ray data; one-chain hexagonal lattice for polymers of $n \leq 8$, and two-chain lattice for polymers of $n \geq 10$ (see text). The measured temperatures are noted close to symbols; no notation means room temperature.

Table II
X-ray Data of Poly(γ-*n*-alkyl L-glutamates)[a]

	Region A		
PG-8-N at 25 °C	PG-14-E at 25 °C	PG-16-E at 25 °C	PG-18-E at 25 °C
	Wide-Angle Region		
14.7 (100) vs			
8.57 (110) s	4.33 (010) vs	4.34 (010) vs	4.37 (010) vs
7.40 (200) m	4.01 (100) s	3.99 (100) s	3.94 (100) s
5.62 (210) m	2.47 (110) m	2.46 (110) m	2.45 (110) m
4.11 (310) vw			
	Low-Angle Region		
6.13 (113) vw	27.2 (100) vs	30.3 (100) vs	32.7 (100) vs
5.69 (203) w	13.7 (200) s	15.2 (200) s	16.4 (200) s
4.73 (213) w	9.18 (300) m	10.1 (300) m	10.9 (300) m
4.62 (115) m	6.85 (400) w	7.53 (400) w	8.10 (400) w
4.39 (205) m		6.08 (500) vw	6.48 (500) vw
2.89 (218) vw			

	Region B			
PG-8-N at 70 °C	PG-10-N at 25 °C	PG-12-N at 25 °C	PG-14-E at 50 °C	PG-16-E at 60 °C
	22.3 (100) s	23.9 (100) vs	25.1 (100) vs	26.7 (100) vs
	13.0 (110) w	13.8 (110) m	14.5 (110) vw	
15.1 (100) vs		11.9 (200) m		
8.72 (110) s		9.05 (210) w		
7.56 (200) w		7.97 (300) vw		
5.72 (210) w				
		5.14 meridonal m		

	Region C			
PG-10-N at 65 °C	PG-12-N at 75 °C	PG-14-E at 90 °C	PG-16-E at 90 °C	PG-18-E at 90 °C
17.5	18.5	20.5	23.0	24.5

[a] Indices are based on the unit cells cited in text.

reduction of densities of the side-chain domain, which would be responsible for the aforementioned decrease of T_β and T_α transition temperatures.

When the temperature is increased, the layer line reflections disappear at a temperature that approximates T_α, whereas the equatorial reflections remain sharp. This can be seen by comparison of the X-ray data of PG-8 at room temperature and at 70 °C listed in the first column on Table II. The same phenomena were observed for PG-5 and PG-6. Such a preferential disappearance of layer line reflections is caused by the translational and librational motions of α-helices with respect to their long axes,[28,29] to which has been attributed the α-relaxation. No essential change of X-ray pattern is observed until 200 °C, where the thermal decomposition becomes noticeable. This leads to the conclusion that no other kind of motion of the main chain has been activated in this experimental temperature range. We thus are led to the view that in this series of polymers there is a consistent variation of packing structure and molecular motion as a simple function of side-chain length.

C. Structure and Properties of PG-*n* for $n \geq 10$. The polymers in this series exhibit two first-order transitions at T_1 and T_2 in place of the β- and α-relaxations. Each transition temperature falls on a smooth curve that increases with side-chain length, as shown in Figure 2. Such a consistent variation of T_1 and T_2 with n indicates that each transition is based on a common structural change for all the polymers in the series. We attempt below to clarify the packing structure and the properties in three temperature regions, A, B, and C, divided by these two curves, as illustrated in Figure 2.

Region A below T_1. The typical X-ray photograph in this region is shown for PG-18 in Figure 4b. The photograph includes two fundamental patterns, one in the wide-angle region which is maintained in some degree throughout the series, and the other in the low-angle region which varies substantially with the length of the side chain. In Table II, these X-ray data are summarized for the polymers in this series where the data of PG-10 and PG-12 have not been included because of low T_1 temperatures.

For PG-18, the pattern in the wide-angle region contains sharp reflections at 4.37, 3.94, and 2.45 Å, as seen in Table II, which can be indexed on a two-dimensional unit cell of a = 4.32 Å, b = 4.79 Å, and γ = 114.3°. With the decrease of the side-chain length, the pattern becomes obscure, but the crystal lattice is only slightly altered: a = 4.39 Å, b = 4.78 Å, and γ = =114.7° for PG-16 and a = 4.32 Å, b = 4.77 Å, and γ = 114.8° for PG-14. These lattices resemble the subunit cell that is attained by c projection of the triclinic unit cell in crystals of polyethylene or low molecular weight n-alkanes.[31-33] Evidently, the side chains have crystallized to form n-alkane type crystals in region A, the melting of which takes place as a first-order transition at T_1. As previously observed in DSC thermograms (Figure 3) the T_1 peak becomes sharp and increases in magnitude with the side-chain length. These data as well as the X-ray data illustrate the effect of increased side-chain length on the development of crystallinity and the perfection of crystals.

The crystallinity can be estimated by DSC calorimetry. In Table III, the transition enthalpy, ΔH_f, and entropy, ΔS_f, per mole of residue are listed, and in Figure 7, ΔH_f is plotted against n. Here, it should be mentioned that the values of ΔH_f and ΔS_f are based on the first heating data of as-cast films. On the second heating after the crystallization at a cooling rate of 10 °C/min, the values are reduced to some extent. This signifies that the side

Table III
Calorimetric Data for Side-Chain Crystals

polymer	ΔH_f, kcal/mol	ΔS_f, cal/mol K	n_c
PG-10-E	0.4	1.6	0.4
PG-12-E	1.3	4.5	1.4
PG-14-E	2.8	8.9	3.0
PG-16-E	5.6	17.1	5.9
PG-18-E	7.3	21.8	7.7

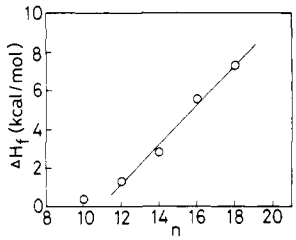

Figure 7. Dependence of the melting enthalpy (ΔH_f) of side-chain crystallites upon n.

chains in the as-cast films have crystallized well in an equilibrium condition through the slow evaporation of solvent during 4 or 5 days. Figure 7 shows that ΔH_f increases with the side-chain length and falls on a line, at least within the range of n = 12–18. Linearity is usually observed for flexible main-chain polymers with the corresponding side-chain crystals[16,17] and is well represented by the equation[34,35]

$$\Delta H_f = \Delta H_{fe} + nk \quad (1)$$

where ΔH_{fe} is a constant reflecting the contribution to the enthalpy due to the chain end and k is the contribution of each added methylene group to the enthalpy. The value of k, evaluated from the solid line of Figure 7, is 0.95 kcal/mol of CH_2. This value is close to the value of 1.0 kcal/mol of CH_2 for the β-triclinic-to-liquid transition exhibited by a homologous series of n-alkanes.[35]

Jordan et al.[16] have revealed that the number of crystalline CH_2 groups in a side chain, n_c, is given by the equation

$$n_c = \Delta H_f/k \quad (2)$$

This equation seems to allow only a rough evaluation of n_c, since some assumptions have been included in its derivation.[16] Despite this fact, it is valuable to present n_c deduced from eq 2, which has been commonly applied in previous studies of side-chain crystals.[16,17,20] These quantities are listed in the last column of Table III. They vary from 0.4 for PG-10 to 7.7 for PG-18. From this it seems that about ten methylene groups in the side chain are in a disordered state, so that only the part of the side chain extending beyond this limit participates in the crystallization. These values of n_c approximate those for flexible main-chain polymers with corresponding n-alkyl side chains.[16,17,20]

It is surprising that there is a good development of crystallinity and perfection of crystals in these particular polymers with side chains projecting from the rigid α-helix. We thus have a question as to how the side chains have become organized to form the crystallites independent of the main-chain conformation. A clue to the answer is offered by the X-ray pattern in the low-angle region. As listed in Table II, the polymers PG-14 to PG-18 exhibit several sharp reflectioins in the low-angle region. The spacings of these reflections increase substantially with the side-chain length. This tendency indicates the attribution of these reflections to the lateral packing array of the

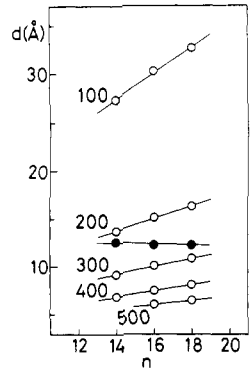

Figure 8. Variation of spacings of $h00$ reflections in the low-angle region with n for polymers of $n \geq 10$ in region A. The closed circles indicate tentative distances between α-helices along the layer.

α-helical chains. We further see in Table II that the patterns contain only a series of reflections with indices of $h00$. Such a unique development of reflections signifies that the main-chain α-helices form a characteristic layer structure in their packing,[7] as shown in Figure 9a, where the individual layer is formed along each 100 plane and the stacking sequence of layers is irregular. In Figure 8, the spacings of the reflections are plotted against n. The spacings of the corresponding reflections increase linearly with n. An increment of the spacing of the 100 reflection, i.e., the layer thickness, is about 1.3 Å per methylene unit of the side chain.

The X-ray pattern provides no information concerning the packing array of the α-helices along a layer because of the lack of $hk0$ reflections. However, the observed densities would allow the calculation of a tentative distance between neighboring chains within each layer since the thickness (the spacing of the 100 reflection) of the layer and the repeat length (27 Å) of the α-helix are known. The observed densities are 1.04_1, 1.04_8, and 1.05_2 g/mL for PG-14, PG-16, and PG-18, respectively. The distances thus calculated are plotted against n in Figure 8. Interestingly, they remain constant around 12.5 Å, which is considerably smaller than the thickness between layers. This result requires that the molecular shape be markedly deformed from cylindrical. For example, the PG-18 molecule has dimensions of 32.7 Å in a direction perpendicular to the layer, in contrast with 12.3 Å along the layer. The latter value approximates the molecular diameter (12 Å) of PG-1. Deformation of molecular shape can thus be understood to occur in such a way that the side chains gather together in two opposite directions so as to fill the space on either side of each layer.

When this characteristic packing array of α-helices is correlated with the side-chain crystals, there is no doubt that the side-chain crystals are located between layers. Hence, the structure is of the comblike type that has been commonly observed for flexible main-chain polymers with side-chain crystallinity.[18-20] This structure is illustrated for PG-18 in Figure 9. Here, the side-chain crystals are shown in such a manner that the side chains protruding from α-helices in neighboring layers intercalate with each other with their axes perpendicular to the layers. For this type of structure, the predicted increment of layer thickness for each additional carbon atom in a side chain is 1.27 Å.[31-33] This value is in good agreement with the experimentally observed increment of 1.3 Å. This also indicates that in polymers the side chains are extended at right angles to the main chain, i.e., the layer. Finally, we can show that the α-helical conformation offers the optimum site for crystallization of side chains so that every side chain is able to participate in crystallization. Figure 9c

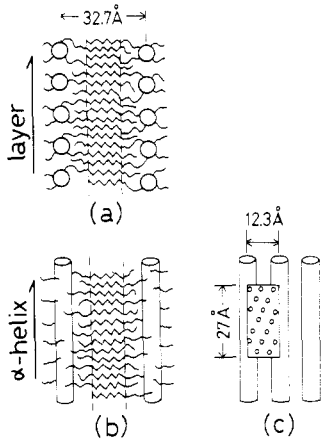

Figure 9. Proposed model of packing structure for PG-18 in region A: (a) viewed parallel to the chain axes of the α-helices; (b) viewed parallel to the layer and perpendicular to the chain axes of the α-helices; (c) viewed perpendicular to both the layer and the chain axes of the α-helices.

illustrates the projection of molecules on the plane perpendicular to the layer, which corresponds to the axial projection with respect to the side-chain crystals. We consider here the number of side chains passing through the unit area defined by the repeating length (27 Å) of the α-helix and the distance (12.3 Å) between molecules along the layer (refer to Figure 9c). The size of the side-chain crystal lattice above elucidated dictates that the number of side chains be around 18 for PG-14, PG-16, and PG-18. This number is exactly equal to the number of side chains that should be located in a unit area. Thus, the crystallization of side chains does not require the distortion of main-chain conformation but the gathering of side chains between layers.

Region B between T_1 and T_2. A typical X-ray photograph in this region is shown for PG-12-N in Figure 4c. At a glance, no existence of side-chain crystals is obvious from the disappearance of reflections in the wide-angle region. The photograph represents the five equatorial reflections attributable to the lateral packing structure of α-helices. They are assigned to the two-dimensional hexagonal lattice with $a = b = 27.6$ Å and $\gamma = 120°$, as listed in Table II. Similar hexagonal packings are observed for other polymers, although the number of reflections has been reduced for the ester-exchange polymers (see Table II).

Apparently, α-helices in this temperature region assume the same kind of packing as those in polymers of the first series. However, we notice that there is a remarkable difference between the two hexagonal packings when we see the n dependence of the spacings of the 100 reflections in Figure 5. Figure 5 shows that there is a discontinuity in the variation of spacing between the two series. The spacings for this series of polymers fall on curve B located above curve A for the first series of polymers. In contrast, Figure 6 illustrates the consistent variation of observed densities with n for the whole series of polymers. This discrepancy in the variation of both parameters can be understood if the two chains are contained in a hexagonal unit cell for polymers with $n \geq 10$; on this assumption, a good correspondence between the calculated and observed densities has been attained, as seen in Figure 6.

It is interesting that the evidence for a larger two-chain unit cell can be seen on the equator of the diffraction pattern, which involves only information about the axial projection of the electron density. This fact signifies that the axial projections of two chains in a unit cell are not equivalent in the crystallographic sense. Here, the explanation that two chains differing in direction (i.e., up and down chains) are contained in a unit cell can be eliminated since these chains are indistinguishable in that projection.[6] In order to satisfy the condition, the two chains are likely to be closely associated by some forces so that they are regarded as a tentative unit chain. We are now considering a structural model in which two chains in a unit cell are in a coiled-coil conformation. This conformation is supported by the simultaneous observation of a 5.13-Å meridional reflection (see Table II), which has been theoretically predicted by Crick.[36] In addition, we have found that the intensity distribution of the equatorial reflections can be explained by a coiled-coil conformation rather than by a single α-helical one.[37] On this point, a detailed examination is in progress.

Region C above T_2. Region C is reached by another first-order transition at T_2. The enthalpy change of this transition is negligibly small and does not vary with n as found in DSC thermograms of Figure 3. In this transition, the X-ray pattern becomes markedly poor; the sharp reflections in region B disappear, being replaced by a broad reflection as typically observed in the photograph of PG-12-N of Figure 4d. Furthermore, Figure 5 shows that the spacings of this reflection are reduced to values that approximate the values expected from the extrapolation of curve A of the polymers in the first series. Hence, the two-chain assembly in region B has disappeared in this region. The dynamic mechanical data of Figure 1b show that the T_2 transition is accompanied by an abrupt drop of the storage modulus E'. As a result, the storage moduli in this region are on the order of 10^7 dyn/cm^2, which is lower than those observed in the final temperature stage around 150 °C for polymers in the first series. Overall characteristics in this region are thus similar to those exhibited by the thermotropic liquid crystalline phases of poly(γ-methyl D-glutamate-*co*-γ-hexyl D-glutamates),[21] indicating that a cholesteric liquid crystal is formed.

As expected from the low storage moduli, the specimens in this region easily flow and spread between glasses under slight stress. In a previous paper on thermotropic copolypeptides,[21] such thin samples showed iridescent colors varying from blue to red with increasing temperature from 150 to 200 °C. These colors have been attributed to cholesteric liquid crystals with pitches comparable to visible wavelengths. Detailed examination of the pitches has been performed by CD measurement. In this system, however, no iridescent colors are observed in the wide temperature range above T_2. We may suppose that the pitches of this system are larger than visible wavelengths, considering that the twisting angles are reduced by the expansion of distance between cholesteric layers due to the long side chains.[38]

In systems with large pitches, the ORD method is useful for determining the pitch P. de Vries[39] predicted that the optical rotatory power, Θ, along the cholesteric helicoidal axis should be given as a function of wavelength λ by

$$\Theta = \frac{-\pi \Delta n^2 P}{4\lambda^2[1 - (\lambda/\lambda_0)^2]} \tag{3}$$

where Δn is the birefringence of an individual cholesteric layer and λ_0 is the $\bar{n}P$ ($\bar{n}$ = average refractive index) at which the optical rotation changes sign. For cholesteric liquid crystals with a large pitch, where $(\lambda/\lambda_0)^2$ is negligibly small, eq 3 can be reduced to

$$\Theta = \frac{-\pi \Delta n^2 P}{4\lambda^2} \tag{4}$$

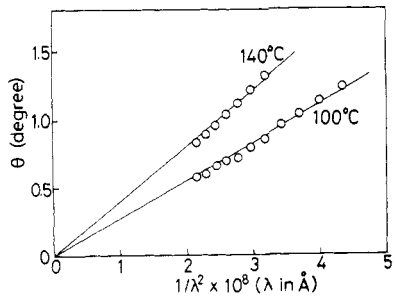

Figure 10. Dependence of the optical rotation upon wavelength for PG-12-N in region C.

This equation indicates that a plot of specific rotation, Θ, vs. $1/\lambda^2$ should give a straight line.

In the present ORD measurements, it should be mentioned that moving the sample cells slightly in the polarimeter so that the light beam passed through different regions of the sample gave a range of rotations. This may be caused partly by a range of cholesteric order and partly by a birefringence effect of the local orientation forcibly induced by spreading the sample between glasses to prepare thin films. In fact, the high molecular weight polymers prepared by the ester-exchange method, in which both effects would be remarkable because of their high viscosities, have exhibited a wide range of rotations and, on some occasions, rotations of opposite sign. For this reason, we have so far obtained reproducible ORD data only for the low molecular weight PG-12-N prepared by the NCA method. In Figure 10, a plot of Θ vs. $1/\lambda^2$ is shown for the ORD data of PG-12-N quenched to room temperature after being annealed at 100 and 140 °C for 12 h. Here, the data were obtained as the average of five measurements for different parts to eliminate the two effects mentioned above. The good linear relationship between Θ and $1/\lambda^2$ can be seen in Figure 10, which confirms the formation of thermotropic cholesteric liquid crystals with large pitches. By the use of the value of $\Delta n = 0.026$,[40] the pitches were calculated to be around 4 and 6 μm at 100 and 140 °C, respectively. In this limited system with a large pitch, the positive optical rotation is equivalent to a negative CD effect so that the cholesteric helix is right-handed for L molecules. This is the same as that observed for L molecules of previous copolypeptides.[21] Furthermore, the temperature dependence of the pitch also appears similar in both cases; increasing temperature causes an increase of pitch.

Concluding Remarks

We have investigated the molecular packing and thermotropic behaviors for a series of poly(L-glutamates) with *n*-alkyl side chains ranging from amyl to octadecyl. In polymers of $n \leq 8$, they were analogous to those of the familiar poly(γ-methyl L-glutamate), varying as a simple function of side-chain length. On the other hand, the polymers of $n \geq 10$ were found to exhibit notable structures and properties.

In the latter polymers of $n \geq 10$, the side chains projecting from the α-helical main chain were crystallizable. The crystallization forced α-helices to pack into a characteristic layer structure, and the crystallites were located between layers, as illustrated in Figure 9. Such a layer structure may possibly result from the growth of crystals in a preferential direction that can effectively produce crystallites of large size. The side-chain crystallites were formed by intercalating side chains protruding from molecules in neighboring layers and contained only a part of the side chain, leaving about ten methylene groups in a disordered state. We believe that the portion of the side chain in the vicinity of the main chain constitutes a disordered phase and an appreciable portion of the end of the side chain interpenetrating into this portion is also disordered. The latter can be supported by the fact that the γ-relaxation, in contrast with the disappearance of the β-relaxation, was still observed irrespective of side-chain crystallization.

The self-crystallization of side chains independent of main-chain asymmetry indicates that the side chain or at least the outer part of it, has achieved a considerable gain in configurational freedom. In other words, the side chains in the melt behave as a liquid paraffin, the motion of which is free from the limitation of the α-helical main chain. In such a system, liquid crystals can be thermally induced, since each α-helix acts as a kinetic unit that can move with some angular freedom around its short axis, as in the lyotropic system. Thus, the crystallization of side chains and the induction of thermotropic liquid crystals may be attributable to the same cause, that is, the solvent nature of the side chain. In fact, the present data have shown the simultaneous appearance of side-chain crystals and liquid crystals for polymers of $n \geq 10$.

It is interesting that the polymers of $n \geq 10$ exhibit another phase between the phase with the side-chain crystals and the liquid crystalline phase. We suggest that in this phase α-helices may assume a coiled-coil structure. The appearance of this conformation is also to be expected considering the solvent nature of the side chains. Parry and Suzuki[41] calculated the interaction energies for various coiled-coil rope models of poly(L-alanine) and found that they are generally more stable than the corresponding straight-chain assemblies. So far, however, synthetic homopolypeptides have never been prepared in a coiled-coil conformation. This stems from the fact that a three-dimensional crystalline arrangement will be more stable since the interrope packing is very poor so that large voids would exist between ropes. Hence, it has only been regarded as a feasible structure in the presence of a suitable solvent to fill the voids. In this sense, the solvent nature of the side chains is likely to favor the coiled-coil structure, although it might not be a direct factor in stabilizing this particular conformation.

The investigation of this series of polymers was initially undertaken with the objective of studying the thermotropic liquid crystalline properties of polypeptides. In this paper, however, no detailed examination of properties has been included because of the limited determination of cholesteric pitches by the ORD method. More recently, we have prepared the poly(γ-benzyl L-glutamate-*co*-γ-dodecyl L-glutamates) with a wide range of compositions. In this system, it was found that thermotropic cholesteric liquid crystals are formed for copolymers with dodecyl contents above 30%, and small pitches, followed by CD measurement, are attained for copolymers with dodecyl contents of 30–70%. In a subsequent paper of this series, a detailed study of the cholesteric properties of these polymers will be described with respect to the dependences of pitch on temperature, thickness of cholesteric layer, and molecular weight.

Registry No. PG-5-E (homopolymer), 52684-40-9; PG-5-E (SRU), 52665-26-6; PG-6-E (homopolymer), 29257-38-3; PG-6-E (SRU), 67422-11-1; PG-8-E (homopolymer), 52684-41-0; PG-8-E (SRU), 52665-27-7; PG-10-E (homopolymer), 4852-92-0; PG-10-E (SRU), 57706-05-5; PG-12-E (homopolymer), 29439-75-6; PG-12-E (SRU), 51949-42-9; PG-14-E (homopolymer), 4958-70-7; PG-14-E (SRU), 98540-57-9; PG-16-E (homopolymer), 4582-72-3; PG-16-E (SRU), 98540-58-0; PG-18-E (homopolymer), 83789-61-1; PG-18-E (SRU), 98540-59-1.

References and Notes

(1) Walton, A. G.; Blackwell, J. "Biopolymers"; Academic Press: New York, 1973.
(2) Fraser, R. D. B.; MacRae, T. P. "Conformation in Fibrous Proteins"; Academic Press: New York, 1973.
(3) Watanabe, J.; Sasaki, S.; Uematsu, I. *Polym. J. (Tokyo)* **1977**, *9*, 451.
(4) Watanabe, J.; Naka, M.; Watanabe, J.; Watanabe, K.; Uematsu, I. *Polym. J. (Tokyo)* **1978**, *10*, 569.
(5) Watanabe, J.; Sasaki, S.; Uematsu, I. *Polym. J. (Tokyo)* **1977**, *9*, 337.
(6) Watanabe, J.; Imai, K.; Gehani, R.; Uematsu, I. *J. Polym. Sci., Polym. Phys. Ed.* **1981**, *19*, 653.
(7) Watanabe, J.; Gehani, R.; Uematsu, I. *J. Polym. Sci., Polym. Phys. Ed.* **1981**, *19*, 1817.
(8) Gehani, R.; Watanabe, J.; Kasuya, S.; Uematsu, I. *Polym. J. (Tokyo)* **1980**, *12*, 871.
(9) Sasaki, S.; Nakamura, T.; Miyamoto, M.; Uematsu, I. *Biopolymers* **1978**, *17*, 2715.
(10) Sasaki, S.; Nakamura, T.; Uematsu, I. *J. Polym. Sci., Polym. Phys. Ed.* **1979**, *17*, 825.
(11) Nagao, M.; Watanabe, J.; Uematsu, I. *Rep. Prog. Polym. Phys. Jpn.* **1980**, *23*, 675.
(12) Watanabe, J.; Sasanuma, Y.; Endo, A.; Uematsu, I. *Polymer* **1984**, *25*, 698.
(13) Watanabe, J.; Uematsu, I. *Polymer*, **1984**, *25*, 1711.
(14) Smith, J. C.; Woody, R. W. *Biopolymers* **1973**, *12*, 2657.
(15) Kaufman, H. S.; Sacher, A.; Alfrey, T.; Frakuchen, I. *J. Am. Chem. Soc.* **1948**, *76*, 6280.
(16) Jordan, E. F., Jr.; Feldeisen, D. W.; Wrigley, A. N. *J. Polym. Sci., Part A-1* **1971**, *9*, 1835.
(17) Jordan, E. F., Jr.; Artymyshyn, B.; Speca, A.; Wrigley, A. N. *J. Polym. Sci.* **1971**, *9*, 3349.
(18) Plate, N. A.; Shibaev, V. P. *J. Polym. Sci., Macromol. Rev.* **1974**, *8*, 117.
(19) Hsieh, H. W. S.; Post, B.; Morawetz, H. *J. Polym. Sci., Polym. Phys. Ed.* **1976**, *14*, 1241.
(20) Gonzalez Dela Campa, J. I.; Barrales-Rienda, J. M.; Gonzalez Ramos, J. *J. Polym. Sci., Polym. Phys. Ed.* **1980**, *18*, 1919, 2197.
(21) Watanabe, J.; Fukuda, Y.; Gehani, R.; Uematsu, I. *Macromolecules* **1984**, *17*, 1004.
(22) Uematsu, Y.; Uematsu, I. In "Mesomorphic Order in Polymers"; American Chemical Society: Washington, DC, **1978**; ACS Symp. Ser. No. 74, p 136.
(23) Kimura, H.; Hashino, M.; Nakano, H. *J. Phys. Soc. Jpn.* **1982**, *51*, 1584.
(24) Yokomori, Y.; Uematsu, Y.; Uematsu, I. *Rep. Prog. Polym. Phys. Jpn.* **1972**, *15*, 633.
(25) Wasserman, D.; Garber, J. D.; Meigs, F. M. U.S. Patent 3 285 953, 1966.
(26) McCrum, N. G.; Read, B. E.; Williams, G. "Anelastic and Dielectric Effects in Polymeric Solids"; Wiley: New York, 1967.
(27) Kajiyama, T.; Kuroishi, M.; Takayanagi, M. *J. Macromol. Sci., Phys.* **1975**, *B11*, 195.
(28) Sasaki, S.; Taguchi, Y.; Kamata, M.; Uematsu, I. *Polymer* **1979**, *20*, 71.
(29) Clark, E. S.; Muus, L. T. *Z. Kristallogr., Kristallgeom., Kristallphys., Kristallchem.* **1962**, *117*, 108, 119.
(30) Fukuzawa, T.; Uematsu, Y.; Uematsu, I. *Polym. J. (Tokyo)* **1974**, *6*, 537.
(31) Teare, P. W.; Holmes, D. R. *J. Polym. Sci.* **1957**, *24*, 496.
(32) Muller, A.; Lonsdale, K. *Acta Crystallogr.* **1948**, *1*, 129.
(33) Turner-Jones, A. *J. Polym. Sci.* **1962**, *62*, S53.
(34) Flory, P. J.; Vrij, A. *J. Am. Chem. Soc.* **1963**, *85*, 3548.
(35) Broadhurst, M. G. *J. Res. Natl. Bur. Stand., Sect. A.* **1962**, *66A*, 241.
(36) Crick, F. H. *Acta Crystallogr.* **1953**, *6*, 685, 689.
(37) Watanabe, J., unpublished data.
(38) Goossens, W. J. A. *Mol., Cryst. Liq. Cryst.* **1971**, *12*, 237.
(39) de Vries, Hl. *Acta Crystallogr.* **1951**, *4*, 219.
(40) Robinson, C.; Ward, J. C. *Nature (London)* **1957**, *180*, 1183.
(41) Parry, D. A. D.; Suzuki, E. *Biopolymers* **1969**, *7*, 189.

Photodegradation of Poly(phenyl vinyl ketones) Containing β-Phenylpropiophenone Moieties[1a]

W. J. Leigh,*[2] J. C. Scaiano,* C. I. Paraskevopoulos,[1b] G. M. Charette, and S. E. Sugamori

Division of Chemistry, National Research Council of Canada, Ottawa, Ontario, Canada K1A 0R6.

Received November 28, 1984

ABSTRACT: The photodegradation of poly(phenyl vinyl ketone) and its copolymers with the methacrylate esters of two para-hydroxy-substituted derivatives of β-phenylpropiophenone (1) was investigated in chlorobenzene solution at 30 °C. Only modest decreases in the photodegradation quantum yields are observed for the copolymers relative to that for poly(phenyl vinyl ketone), and this is rationalized in terms of structural constraints on the energy-transfer process. These result from the fact that the β-phenylpropiophenone moieties are held at considerable distances from their nearest-neighbor benzoyl groups on the polymer backbone, distances that are too large for efficient triplet energy transfer to take place. The relative effectiveness with which the isomeric methacrylate esters stabilize the polymer is consistent with the predominance of an intracoil quenching mechanism. The parent substrate, 1, quenches phenylalkyl ketone triplets with a rate constant of $k_q = 1.7 \times 10^9$ M^{-1} s^{-1} in benzene solution at room temperature.

Introduction

The photodegradation of aromatic ketone-based polymers, e.g., poly(phenyl vinyl ketone) (pPVK, eq 1), has been the subject of numerous investigations.[3-9] These polymers are known to undergo photodegradation primarily via the Norrish II reaction from the triplet manifold.[5,6a]

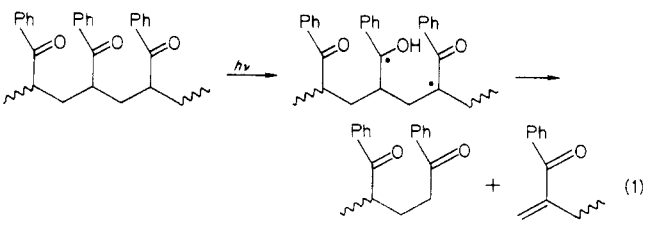

The initial quantum yield for photodegradation of pPVK is ca. 0.24;[5,6a,8d,9b] the efficiency of this process decreases rapidly as photodegradation proceeds as a result of the accumulation of α,β-unsaturated ketone end groups, which act as efficient triplet quenchers.[8b]

Laser flash photolysis studies have unraveled many of the mechanistic details pertaining to the photodegradation of polymers of this type. The triplet lifetime in carefully purified samples (τ = 55 ns)[9c,10] is a factor of ca. 20 longer than that of monomeric phenylalkyl ketones capable of intramolecular γ-hydrogen abstraction, such as γ-methylvalerophenone,[11] which may reflect the decreased mobility of the benzoyl group with respect to γ-hydrogens in the polymer. Furthermore, since energy migration in these polymers has been shown to reduce their rate of

0024-9297/85/2218-2148$01.50/0 Published 1985 by the American Chemical Society